Activation of Atomic Transport via Vibrational Coupling-Induced Force Fluctuations

Yechan Noh1 and N. R. Aluru2, a)

¹Department of Mechanical Science and Engineering, University of Illinois at Urbana-Champaign, Urbana, Illinois 61801, United States

²Walker Department of Mechanical Engineering, Oden Institute for Computational Engineering and Sciences, The University of Texas at Austin, Austin 78712, United States

^{a)}Author to whom correspondence should be addressed: aluru@utexas.edu

KEYWORDS

Vibrational coupling, Mass transport, Nanopore, Natural frequency, Frequency match, Transport barrier, Fluctuating force.

ABSTRACT

Vibrational coupling, although well-explored in many fields, has seldom been investigated in the context of mass transport. In this letter, we examine the impact of vibrational coupling on atomic transport using simple molecular dynamics simulations. Our study shows that the atomic transport can be activated when the natural frequency of the atomic slit is close to the natural frequency of the atom being transported. We uncover the presence of fluctuating forces induced by vibrational coupling, with higher amplitudes observed when the coupling is strong. We show that the transport activation mechanism is due to the high force fluctuations that arise during strong vibrational coupling allowing the atom to temporarily surpass the transport barrier of the slit. Our findings will serve as a foundation for the continued examination of vibrational coupling in the realm of mass transport.

At the molecular scale, all matter vibrates and coupling between matter can give rise to interesting physical phenomena. For example, in the field of energy transfer, the inter-molecular vibrational coupling serves as an efficient route for energy transfer^{1,2}. In the field of chemistry, vibrational coupling between the substance and photon has been demonstrated to modify the reaction selectivity^{3,4} opening massive possibilities to control chemical reactions. Additionally, vibrational coupling plays an important role in protein dynamics⁵, vibrational spectroscopy⁶, and interfacial heat transfer⁷. Despite its relevance in various fields, vibrational coupling is a relatively unexplored concept in the realm of nanoscale mass transport.

Microscopic mass transport is a vital process in living systems to operate numerous functionalities such as delivering nutrition, transferring neurotransmitters, and regulating homeostasis⁸. During the last few years, artificial nanofluidic devices have received significant attention due to their attractive properties in electricity generation⁹, energy storage¹⁰, water purification^{11,12}, and molecular separation¹³. Moreover, recent progress in nanopore fabrication techniques has led to the production of large-scale two-dimensional nanoporous materials with uniform pore sizes^{14,15} contributing to innovative nanofluidic applications. The critical length scale in interesting nanofluidic applications ranges from a few Angstroms to several tens of Angstroms. The fluctuations/vibrations of nanofluidic devices can be comparable to the critical length scale and this can impact nanoscale transport [16]. However, there is a lack of fundamental understanding of how mass transport is influenced by vibrational coupling between the solid media (nanofluidic channel/pore) and the fluid media being transported.

There have been previous reports indicating the relationship between vibrational coupling and the diffusion of fluids. In 2015, Ma *et al.*¹⁷ conducted molecular dynamics (MD) simulations and found that the diffusion of water molecules in a carbon nanotube increased by more than 300%

due to the longitudinal phonon mode of nanotube. The theory proposed by Marbach et al. 18 suggests that the effective diffusion of fluids within a wiggling channel can be either enhanced or reduced depending on the spectrum of surface fluctuations. Noh and Aluru 19 performed MD simulations and reported a two-fold faster water desalination due to vibrational coupling between water and membrane. Their subsequent work 16 showed that vibrational coupling becomes increasingly influential in smaller pores (water flow increases up to 500 % in a 0.75 nm diameter pore). MD simulations performed by Lyu et al. 20 show increased ion conductivity in a flexible covalent organic framework membrane, which better aligned with experimentally measured ion conductivity. Despite these previous reports, the fundamental physical mechanism behind the enhancement of mass transport through vibrational coupling remains largely unknown.

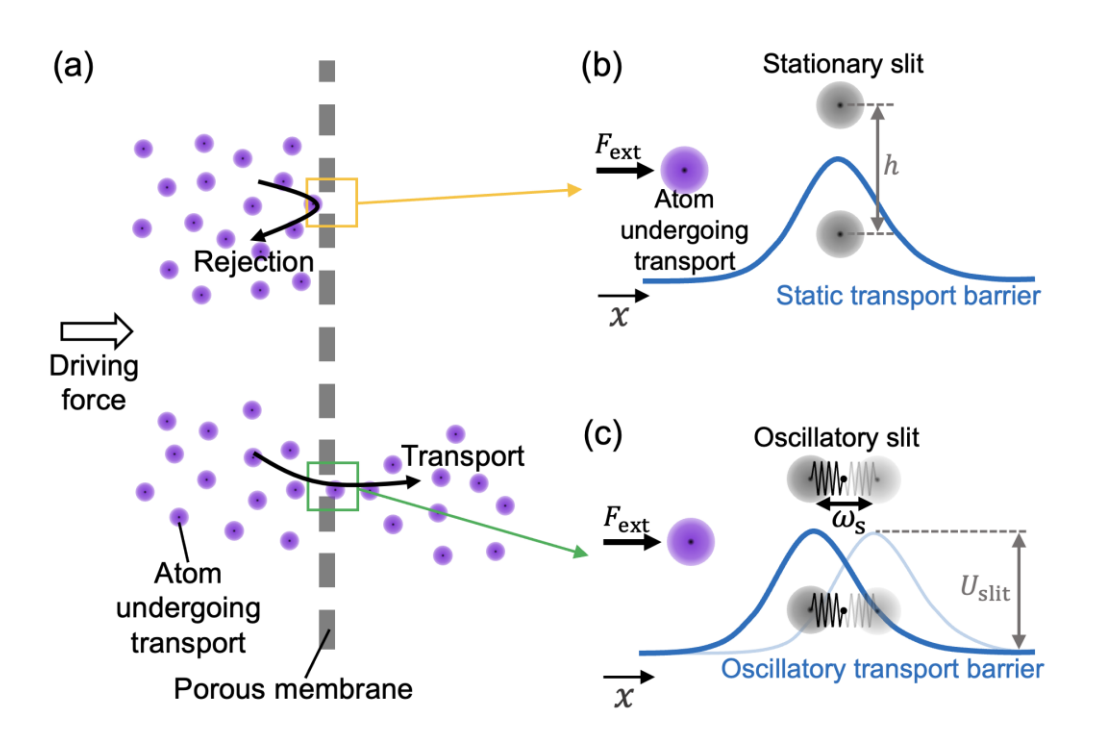


FIG. 1. Illustrative representation of systems for atomic transport through oscillatory slits.

(a) An illustration of atomic transport and rejection in a porous membrane (b) A stationary slit. (c)

An oscillatory slit, in which a spring is attached between the slit atom and a fixed point. The blue

line denotes the transport barrier of the slit. F_{ext} is the force exerted on the atom undergoing transport, h is the separation of slit, U_{slit} is the transport barrier of slit.

To investigate the effect of vibrational coupling on microscopic mass transport phenomena, as illustrated in Fig. 1(a), we designed simple molecular dynamics simulations consisting of one atom being transported and two slit atoms. This setup forms a straightforward, yet an effective model, to clearly demonstrate the vibrational coupling effect in the atomic transport process. We considered two different cases: one being a stationary slit with a fixed position (see Fig. 1(b)), and the other being an oscillatory slit, where the slit oscillates (see Fig. 1(c)). For microscopic oscillations of slit, springs are attached between the slit atoms and fixed points. The slit is restricted to move only along the x-coordinate for the sake of simplicity. The interatomic force was modeled using the Lennard-Jones (LJ) potential with a cutoff distance of 25 Å. The LJ parameters were taken to be $\sigma=3.39$ Å and $\epsilon=0.0692$ Kcal/mol for the slit atoms and $\sigma=2.50$ Å and $\epsilon=0.0692$ Kcal/mol for the slit atoms and $\sigma=0.0692$ Kcal/mol for the slit atoms at $\sigma=0.0692$ Kcal/mol for $\sigma=0.069$ 0.0300 Kcal/mol for the representative fluid atom undergoing transport. The cross-interaction LJ parameters were calculated using the Lorentz-Berthelot mixing rule. The atomic mass is set to be 1 g/mol for the atom undergoing transport and 12 g/mol for the slit atom. The separation of slit size is 4.9 Å (center-to-center distance) and the initial distance between the center of slit and the atom undergoing transport was set at 4 Å. The initial Hamiltonian of the slit atom is set to be $2k_BT$, where k_B is the Boltzmann constant and T is the temperature (298 K in this work). The time step for the simulation was set at 1 fs, and the atomic trajectories were calculated under the microcanonical ensemble using Large-scale Atomic/Molecular Massively Parallel Simulator²¹. We considered various natural frequencies of the slit (5 cm⁻¹ $\leq \omega_s \leq$ 1000 cm⁻¹) by adjusting

the spring constant. The natural frequency of the slit ω_s is determined by the spring constant and the mass of the slit atom, which is given by the formula $\omega_s = \frac{1}{2\pi c_0} \sqrt{\frac{k}{m_s}}$ in units of 1/distance, where c_0 is the speed of light in vacuum, k is the spring constant, and m_s is the mass of the slit atom. For comparison, we also considered a stationary (immobile) slit where the vibrational coupling is absent.

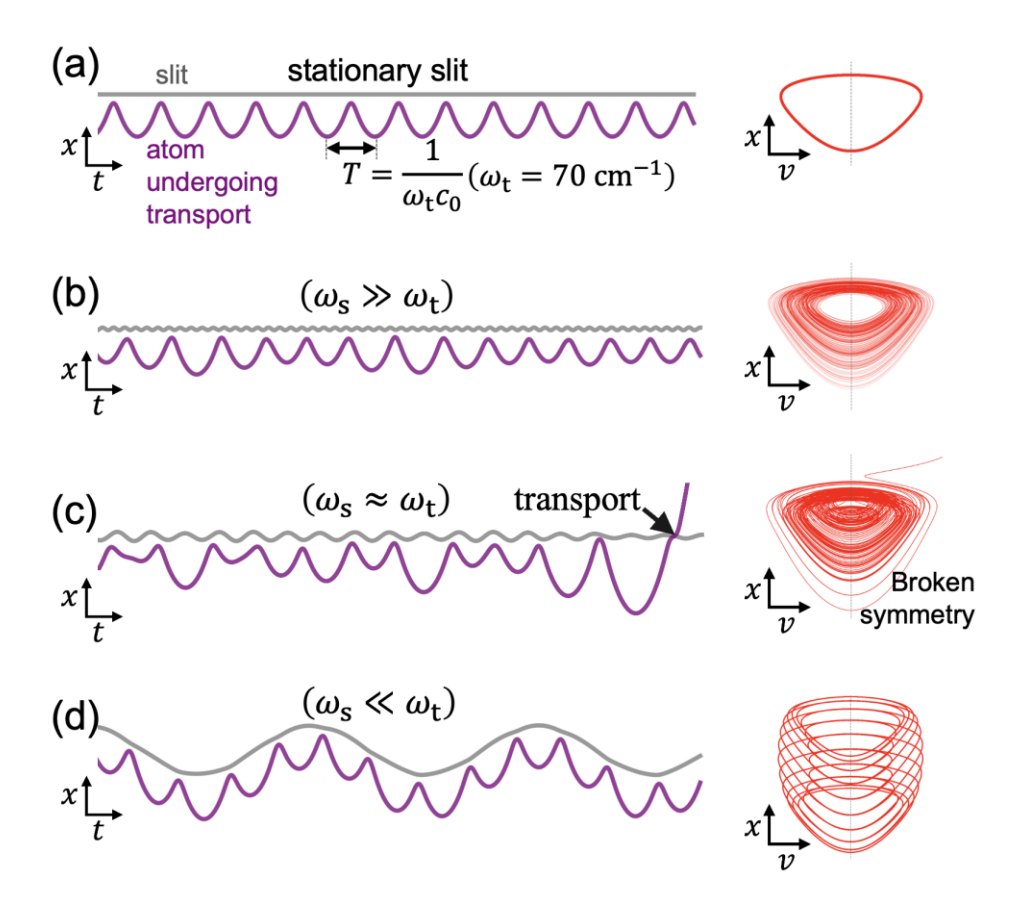


FIG. 2. Alterations of atomic trajectories and x-v phase plot due to the vibrational coupling. Atomic trajectories (left) and x-v phase plot (right) are depicted for (a) a stationary slit, (b) a high frequency slit, (c) a near-critical frequency slit, and (d) a low frequency slit. T is the period of the

trajectory. ω_t and ω_s are the natural frequencies of the atom undergoing transport and the slit, respectively. c_0 is the speed of light in vacuum.

To investigate transport of the representative fluid atom (simply referred to as the atom in the rest of the discussion), we exerted a constant force of 0.02084 nN on the atom. Fig. 2(a) shows the trajectories of atoms and the stationary slit. The atom approaches the slit due to the external force. However, the external force is insufficient to surmount the transport barrier of the slit, created by the repulsive LJ potential. As a result, the atom bounces back from the slit and oscillates at the entrance of the slit creating motions in the 2D plane. In the absence of vibrational coupling (i.e., in the stationary slit case), the atom exhibits periodic oscillations, resulting in a simple closed loop in the x-v phase plot, which is symmetric with respect to the velocity axis. The natural frequency of the atom undergoing transport ω_t can be calculated from the trajectory as $\omega_t = \frac{1}{Tc_0}$ in units of 1/distance, where T is the period of the trajectory. The frequency was calculated to be $70~\text{cm}^{-1}$, equivalent to 2.1 THz, with an amplitude of 3.17 Å for the parameters used in the present study. In contrast, the presence of vibrational coupling (i.e., oscillatory slit case), introduces additional complexity in trajectories and the x-v phase plot as shown in Fig. 1. This effect becomes greater when the natural frequencies of the slit and atom are close to each other. Notably, we found that the vibrational coupling can activate atomic transport. Specifically, in the case of strong vibrational coupling (i.e., the natural frequencies are close to each other, $\omega_s \approx \omega_t$), the atom was able to overcome the transport barrier of the slit, breaking the symmetry of the x-v phase plot. On the other hand, when the vibrational coupling is weak (i.e., $\omega_s \ll \omega_t$ or $\omega_s \gg \omega_t$) the atom was unable to surmount the transport barrier of slit and the x-v phase plot remains symmetric with respect to the velocity axis. This result highlights that the vibrational properties of materials are a crucial factor for microscopic mass transport. Also, the transport of an oscillating atom involves non-linear symmetry breaking phenomena. We note that a similar behavior was observed for a forced oscillation where the slit oscillates with a predefined sine function. This suggests that the use of external means of vibrations, such as photons, can modulate the microscopic mass transport. In fact, modulating chemical reactions and the state of matter using light-matter vibrational coupling has been actively studied^{3,22–25}. Further investigations are needed to explore the feasibility of altering microscopic transport through light-matter vibrational coupling as this could have significant implications for a range of fields, including materials science, chemistry, and nanotechnology.

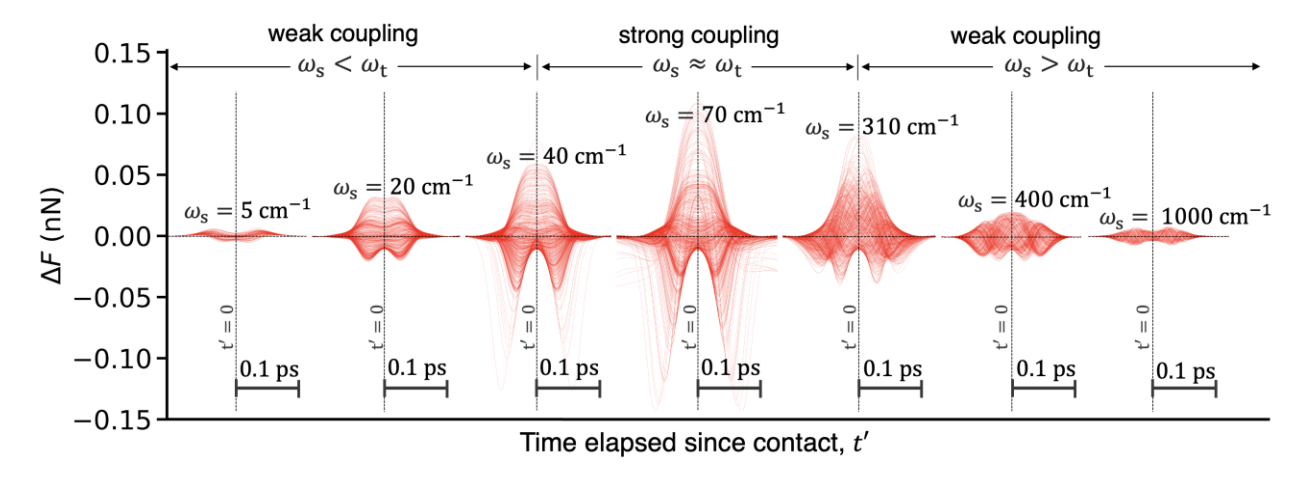


FIG. 3. Vibrational coupling-induced force ΔF and its fluctuation for different natural frequencies of the slit. The red lines represent superimposed ΔF for various contacts. ω_s and ω_t are the natural frequencies of the slit and the atom undergoing transport, respectively. In this case study, ω_t is fixed at 70 cm⁻¹.

To gain a deeper understanding of the underlying physical mechanisms, we analyzed the dynamics of force for over 100 different initial positions of the slit for each frequency. We computed the forces acting on the atom from the slit. Then, the force difference ΔF , referred to as the vibrational coupling-induced force, was obtained using the formula $\Delta F(t') = F_{\omega}(t-t_{\omega})$ – $F_0(t-t_0)$, where F_{ω} and F_0 are the forces acting on the atom from oscillatory and stationary slit respectively, t' is time elapsed since contact, t_{ω} and t_0 are the time of contact in oscillatory and stationary slit, respectively, defined as the moment when the atom is closest to the slit. We superimposed the force difference for various contacts and plotted the results in Fig. 3. The vibrational coupling-induced force ΔF exhibits fluctuations for different contacts and its amplitude and shape vary depending on the natural frequency of the slit (the natural frequency of the atom is fixed). Importantly, the amplitude of ΔF is maximum when the natural frequency of the slit matches with the natural frequency of the atom. This effect is attributed to the enhanced momentum exchange between the atom and the slit when their frequencies match. The momentum flux can be written as $\frac{dM}{dt} = \frac{dm}{dt}\frac{dx}{dt} + m\frac{d^2x}{dt^2}$, where M is the momentum and m is the mass. For the system where the time derivative of mass is zero $\left(\frac{dm}{dt} = 0\right)$, the force is equivalent to the momentum flux as $F = m \frac{d^2x}{dt^2} = \frac{dM}{dt}$. Thus, in our system the fluctuations of ΔF are equivalent to the fluctuations of vibrational coupling-induced momentum flux between the atom and the slit. Thus, the augmented fluctuations under the strong vibrational coupling can be understood as the result of enhanced momentum exchange when the natural frequencies match. Besides, the diminishing fluctuations of ΔF at low and high frequencies can be rationalized by considering the low and high frequency limits. At the high frequency limit, the slit behaves like a stationary slit as it is anchored by an infinitely stiff spring and vibrates with an infinitesimal amplitude and an infinitely high frequency. On the other hand, at the low frequency limit, the velocity of the slit is almost invariant with respect to time. As the atom moves in conjunction with the slit, the atom hardly perceives the motion of the slit according to the equivalence principle. As a result, a slit oscillating at high and low frequency limit has a negligible impact on the dynamics of the atom.

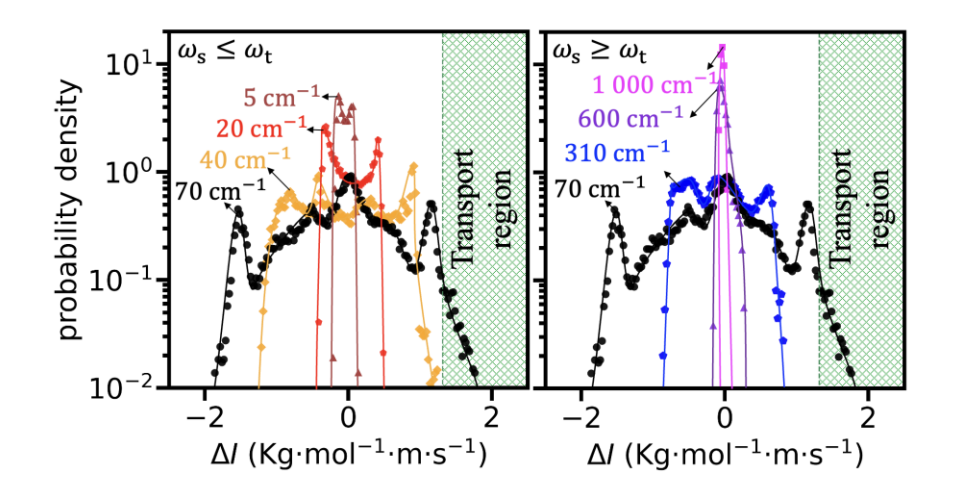


FIG. 4. Distribution of vibrational coupling-induced impulse ΔI for different frequencies of the slit. (left) low frequency slits ($\omega_s \leq \omega_t$) and (right) high frequency slits ($\omega_s \geq \omega_t$). The green grid area represents transport region ($\Delta I \geq I_{\rm th} - I_0$). ΔI is the time integration of ΔF that represent momentum exchange caused by vibrational coupling (specific formula can be found in the main text). $I_{\rm th}$ is the threshold impulse that is needed to surmount the transport barrier of the slit $U_{\rm slit}$, which is given by $I_{\rm th} = \sqrt{2m_t U_{\rm slit}}$, where m_t is the mass of the atom undergoing transport and I_0 is the impulse obtained from the stationary slit case.

Next, we will further delve deeper into how a fluctuating force with zero-mean activates the atomic transport. The time integration of ΔF characterizes the momentum exchange caused by

vibrational coupling: $\Delta I = \int_{t_{\rm BC}}^{t_{\rm AC}} \Delta F \, dt$, where $t_{\rm BC}$ and $t_{\rm AC}$ are before and after contact, respectively, that are the moments when the atom is farthest from the slit. The probability distributions of ΔI are shown in Fig. 4. ΔI has zero mean and its distribution becomes wider when the natural frequency of slit matches that of the atom. The distribution of ΔI exhibits multiple peaks with complicated shapes and do not follow a well-defined distribution such as a Gaussian or a Poisson distribution. ΔI is also a fluctuating quantity that changes from one collision to another. The fluctuations of ΔI can activate the atomic transport by allowing the atom to momentarily overcome the transport barrier of the slit. Recall the fact that transport occurs when vibrational coupling is strong where the distribution of ΔI is wider. This implies that there is a specific limit of ΔI for transport. To determine this limit, we calculated a threshold impulse $I_{\rm th}$ that corresponds to the transport barrier of slit, which is given by $I_{\rm th}=\sqrt{2m_{\rm t}U_{\rm slit}}$, where $m_{\rm t}$ is the mass of the atom undergoing transport and $U_{\rm slit}$ is the transport barrier of slit. Using that and the impulse in stationary slit I_0 , we identify the transport region given by $\Delta I \ge I_{\rm th} - I_0$ (See Fig. 4.). This suggests that transport is activated when the vibrational coupling creates ΔI that is higher than $I_{\rm th}-I_{\rm 0}$. This analysis is consistent with our simulation data where the atomic transport is activated for $\omega_{\rm s}=70~{\rm cm^{-1}}$ where ΔI lies within the transport region. Thus, the physical mechanism behind the transport activated by vibrational coupling is that the vibrational coupling creates fluctuations of exchanged momentum between the slit and the atom undergoing transport. This fluctuation provides changes for the atom to momentarily surmount the transport barrier of the slit.

In summary, our study demonstrates the activation of atomic transport in Angstrom-scale slits through vibrational coupling between the slit and the atom and revealed the underlying

physical mechanism. We found that atomic transport is activated when a slit vibrates with a certain range of frequencies. By comparing the forces exerted from the stationary slit and oscillatory slit, we reveal the existence of force induced by vibrational coupling. This vibrational coupling-induced force exhibits temporal fluctuations, and its amplitude is maximized when the natural frequency of the slit matches that of the atom undergoing transport. This effect is due to the high rate of momentum exchange between the atom and the slit when their natural frequencies match. We analyzed the momentum change caused by vibrational coupling (the vibrational coupling-induced impulse ΔI). Remarkably, vibrational coupling widens the distribution of ΔI and affords the atom with an opportunity to momentarily overcome the transport barrier of the slit. These findings contribute to the understanding of vibrational coupling in the realm of mass transport and lays the foundations for future investigations in this field. We remark that this work has farreaching implications for modulating and engineering microscopic mass transport using vibrational coupling.

ACKNOWLEDGMENTS

The work was supported by the Center for Enhanced Nanofluidic Transport (CENT), an Energy Frontier Research Center funded by the U.S. Department of Energy, Office of Science, Basic Energy Sciences (Award # DE-SC0019112). All other aspects of this work were supported by the National Science Foundation under Grants 2140225 and 2137157. The computing power is provided by the Extreme Science and Engineering Discovery Environment (XSEDE) granted by National Science Foundation (NSF) Grant No. OCI1053575 and Blue Waters supercomputing center, awarded by the state of Illinois and NSF, OCI-0725070, ACI-1238993.

AUTHOR DECLARATIONS

Conflict of Interest

The authors have no conflicts to disclose.

Author Contributions

N. R. Aluru: Conceptualization (lead); Funding acquisition (lead); Project administration (lead); Resources (equal); Supervision (lead); Writing – review & editing (equal). **Yechan Noh:** Formal analysis (lead); Investigation (lead); methodology (lead); Resource (equal); Software (lead); Visualization (lead); Writing – original draft (lead); Writing – review & editing (equal).

Data Availability

The data that support the findings of this study are available from the corresponding author upon reasonable request.

REFERENCES

- ¹ S. Woutersen, and H.J. Bakker, "Resonant intermolecular transfer of vibrational energy in liquid water," Nature **402**(6761), 507–509 (1999).
- ² C.-C. Yu, K.-Y. Chiang, M. Okuno, T. Seki, T. Ohto, X. Yu, V. Korepanov, H. Hamaguchi, M. Bonn, J. Hunger, and Y. Nagata, "Vibrational couplings and energy transfer pathways of water's bending mode," Nat Commun **11**(1), 5977 (2020).
- ³ A. Thomas, L. Lethuillier-Karl, K. Nagarajan, R.M.A. Vergauwe, J. George, T. Chervy, A. Shalabney, E. Devaux, C. Genet, J. Moran, and T.W. Ebbesen, "Tilting a ground-state reactivity landscape by vibrational strong coupling," Science **363**(6427), 615–619 (2019).
- ⁴ H. Frei, L. Fredin, and G.C. Pimentel, "Vibrational excitation of ozone and molecular fluorine reactions in cryogenic matrices," J. Chem. Phys. **74**(1), 397–411 (1981).
- ⁵ K.A. Henzler-Wildman, M. Lei, V. Thai, S.J. Kerns, M. Karplus, and D. Kern, "A hierarchy of timescales in protein dynamics is linked to enzyme catalysis," Nature **450**(7171), 913–916 (2007).
- ⁶ B.C. Stipe, M.A. Rezaei, and W. Ho, "Single-Molecule Vibrational Spectroscopy and Microscopy," Science **280**(5370), 1732–1735 (1998).
- ⁷ J. Chen, X. Xu, J. Zhou, and B. Li, "Interfacial thermal resistance: Past, present, and future," Rev. Mod. Phys. **94**(2), 025002 (2022).
- ⁸ K. Kunzelmann, "Ion Channels and Cancer," J Membrane Biol **205**(3), 159–173 (2005).
- ⁹ J. Feng, M. Graf, K. Liu, D. Ovchinnikov, D. Dumcenco, M. Heiranian, V. Nandigana, N.R. Aluru, A. Kis, and A. Radenovic, "Single-layer MoS2 nanopores as nanopower generators," Nature **536**(7615), 197 (2016).
- ¹⁰ A.K. Mandal, J. Mahmood, and J.-B. Baek, "Two-Dimensional Covalent Organic Frameworks for Optoelectronics and Energy Storage," ChemNanoMat **3**(6), 373–391 (2017).
- ¹¹ D. Cohen-Tanugi, and J.C. Grossman, "Water Desalination across Nanoporous Graphene," Nano Lett. **12**(7), 3602–3608 (2012).
- ¹² Y. Yang, X. Yang, L. Liang, Y. Gao, H. Cheng, X. Li, M. Zou, R. Ma, Q. Yuan, and X. Duan, "Large-area graphene-nanomesh/carbon-nanotube hybrid membranes for ionic and molecular nanofiltration," Science **364**(6445), 1057–1062 (2019).
- ¹³ X.Q. Cheng, Z.X. Wang, X. Jiang, T. Li, C.H. Lau, Z. Guo, J. Ma, and L. Shao, "Towards sustainable ultrafast molecular-separation membranes: From conventional polymers to emerging materials," Progress in Materials Science **92**, 258–283 (2018).
- ¹⁴ Y. Zhong, B. Cheng, C. Park, A. Ray, S. Brown, F. Mujid, J.-U. Lee, H. Zhou, J. Suh, K.-H. Lee, A.J. Mannix, K. Kang, S.J. Sibener, D.A. Muller, and J. Park, "Wafer-scale synthesis of monolayer two-dimensional porphyrin polymers for hybrid superlattices," Science **366**(6471), 1379–1384 (2019).
- ¹⁵ J. Bai, X. Zhong, S. Jiang, Y. Huang, and X. Duan, "Graphene nanomesh," Nature Nanotech **5**(3), 190–194 (2010).
- ¹⁶ Y. Noh, and N.R. Aluru, "Effect of interfacial vibrational coupling on surface wettability and water transport," Phys. Rev. E **106**(2), 025106 (2022).
- ¹⁷ M. Ma, F. Grey, L. Shen, M. Urbakh, S. Wu, J.Z. Liu, Y. Liu, and Q. Zheng, "Water transport inside carbon nanotubes mediated by phonon-induced oscillating friction," Nature Nanotechnology **10**(8), 692–695 (2015).
- ¹⁸ S. Marbach, D.S. Dean, and L. Bocquet, "Transport and dispersion across wiggling nanopores," Nature Physics **14**(11), 1108–1113 (2018).

- ¹⁹ Y. Noh, and N.R. Aluru, "Phonon-Fluid Coupling Enhanced Water Desalination in Flexible Two-Dimensional Porous Membranes," Nano Lett. **22**(1), 419–425 (2022).
- ²⁰ B. Lyu, M. Wang, Z. Jiang, and J. Jiang, "Microscopic insight into anion conduction in covalent-organic framework membranes: A molecular simulation study," Journal of Membrane Science **658**, 120754 (2022).
- ²¹ S. Plimpton, "Fast Parallel Algorithms for Short-Range Molecular Dynamics," Journal of Computational Physics **117**(1), 1–19 (1995).
- ²² F.J. Garcia-Vidal, C. Ciuti, and T.W. Ebbesen, "Manipulating matter by strong coupling to vacuum fields," Science **373**(6551), eabd0336 (2021).
- ²³ K. Nagarajan, A. Thomas, and T.W. Ebbesen, "Chemistry under Vibrational Strong Coupling," J. Am. Chem. Soc. **143**(41), 16877–16889 (2021).
- ²⁴ D. S. Dovzhenko, S. V. Ryabchuk, Y. P. Rakovich, and I. R. Nabiev, "Light–matter interaction in the strong coupling regime: configurations, conditions, and applications," Nanoscale **10**(8), 3589–3605 (2018).
- ²⁵ J. George, A. Shalabney, J.A. Hutchison, C. Genet, and T.W. Ebbesen, "Liquid-Phase Vibrational Strong Coupling," J. Phys. Chem. Lett. **6**(6), 1027–1031 (2015).